

THE MOLECULAR CLOUD RING IN NGC 1068

STEVEN T. MYERS AND N. Z. SCOVILLE

California Institute of Technology

Received 1986 August 25; accepted 1986 October 27

ABSTRACT

The Owens Valley Millimeter Interferometer has been used to map the CO emission in the nucleus of NGC 1068 at 6'' resolution (500 pc). Approximately 50% of the total CO emission within the central 6 kpc is contained in a ring (or arms) at $R = 0.9\text{--}2.4$ kpc near the outer edge of the inner disk where infrared observations have shown a high rate of massive star formation. The CO kinematics indicate mean circular and expansion velocities of 164 and 71 km s^{-1} , respectively for the ring assuming a major axis position angle of 55° . (For a major axis PA = 82° , the circular velocity is 185 km s^{-1} and the expansion velocity is $< 20 \text{ km s}^{-1}$.) The mass of molecular clouds within this region is approximately $4 \times 10^9 M_\odot$. It is proposed that the ring has formed of gas collected by the action of a central stellar bar; the infall of this gas may have been triggered by a close encounter or merger with another galaxy.

Subject headings: galaxies: nuclei — interstellar: molecules — stars: formation

I. INTRODUCTION

Optical and infrared studies over the last decade have revealed intense bursts of star formation activity occurring in the nuclei of a small fraction of the spiral galaxies. The recent *IRAS* survey detected a number of galaxies with total far infrared luminosities exceeding $10^{12} L_\odot$; several appear to be interacting pairs of galaxies (Soifer *et al.* 1986; Sanders *et al.* 1986). Although most of the distant higher luminosity *IRAS* galaxies have yet to be studied in detail, several of them also show signs of both AGN and starburst activity. The existence of both an active nucleus and regions of enhanced star formation suggests the possibility of a causal link or, at least, a circumstantial relationship between the two phenomena.

The SB spiral galaxy, NGC 1068, is one of the nearest Seyfert galaxies (type II) located at a distance of 18.1 Mpc (Sandage and Tammann 1975); it is perhaps the nearest example of a galaxy with both a high rate of star formation and an active nucleus. It has been mapped at high resolution in the radio, infrared, and optical wavelengths, and at lower resolution in the millimeter line of CO. These observational studies have revealed two distinct angular scales over which the activity occurs—a core $< 3''$ in radius, and a nuclear disk extending out to radius $20''$. A total far-infrared luminosity of $3 \times 10^{11} L_\odot$ originates from the central $30''$ of the galaxy, approximately 50% in the core source (< 100 pc) and 50% in a 3 kpc diameter disk. The latter component is most likely due to an extended disk of high-mass star formation (Telesco *et al.* 1984). VLBI and VLA imaging of the radio continuum revealed a central nonthermal source < 1.5 pc in diameter, coincident with the infrared core in addition to two opposing jets extending approximately $10''$ along the major axis (Wilson and Ulvestad 1983; Ulvestad, Neff, and Wilson 1986).

Direct evidence for a dense, interstellar medium in the nuclear region of NGC 1068 is provided by single-dish measurements of the 2.6 mm CO line. Scoville, Young, and Lucy (1983) estimate a mass of $6 \times 10^9 M_\odot$ for the molecular

clouds (H_2 and He) within the central 3 kpc disk (for a distance of 18.1 Mpc). Although their measurements had insufficient resolution ($50''$) to resolve the gas distribution relative to the nuclear activity, they analyzed the line profiles to deduce the presence of a ringlike structure in the molecules at $10''\text{--}15''$ radius. In this *Letter*, we report high-resolution interferometric measurements of the CO emission from NGC 1068 at resolution $\sim 6''$ which verify the existence of the molecular gas ring and enable us to measure the neutral gas kinematics independently.

II. OBSERVATIONS

The observations were made during 1986 May–June with the Owens Valley Radio Observatory (OVRO) three-element millimeter-wave interferometer. Each of the 10.4 m telescopes was equipped with a SIS receiver cooled to 4.5 K. Measured receiver temperatures were approximately 300 K SSB. Spectral coverage was provided by a filterbank consisting of 32.5 MHz channels giving a coverage of 416 km s^{-1} at a resolution of 13 km s^{-1} in the CO $J = 1\text{--}10$ transition. NGC 1068 was observed in five configurations with baselines out to 55 m east-west and 80 m north-south. The corresponding synthesized, untapered beam was $5''$ (N–S) by $7''$ (E–W). The primary field of view of the telescopes is $\sim 70''$.

Phase calibration of the interferometer was accomplished by observing the standard point sources (0420–014 and 0106+013) every half hour. Corrections for receiver gain and sky opacity variations were derived from measurements of an ambient temperature chopper wheel at the beginning of each 5 minute integration on the source. The absolute flux scale was established from observations of 3C 84 which was related to Uranus ($T_B = 134$ K; Ulich 1981).

Interferometer data were processed after initial calibration using the NRAO AIPS package. The noise in the resulting maps was within a factor of 2 of the expected thermal

1987ApJ...312...39M

fluctuation level of 140 mJy. Since the shortest projected baseline possible with the interferometer is 10 m (corresponding to 30"), emission extended over greater angular scales is absent from our data. No single-dish measurements or zero spacing flux were introduced in the maps to offset this effect. In addition to the full-resolution maps (5" x 7"), a 12 kλ taper was applied to the *w* data to generate maps with higher sensitivity but lower resolution (7" x 11"). All maps were corrected for the falloff in the primary beam response.

III. RESULTS

In Figure 1 (Plate L2), the CO interferometer image is shown in conjunction with the optical and radio continuum emission. In Figure 2, the CO centroid velocities are superposed on the 7" x 11" resolution CO emission contours. The total integrated CO line flux in the interferometer maps corresponds to approximately 50% of that observed in a 60" resolution single-dish measurement (Scoville, Young, and Lucy 1983). Thus, there must be some low surface brightness emission from distributed gas outside the structures shown in the maps.

The dominant emission peaks are located symmetrically north and south of the nucleus at distances of 14", but extended emission (most evident in the low-resolution map, Fig. 2) almost completely encircles the nucleus. The two largest concentrations coincide closely with dust lanes seen visually at the edge of the bright inner disk (see Fig. 1a). In the following discussion, we refer to this structure as a ring although it could equally well be two spiral arms. Assuming an inclination of 40° for NGC 1068, the deprojected mean

radius of the ring is 1.6 kpc. The peak single-channel flux (2 Jy per [5" x 7" beam]) corresponding to a mean brightness temperature of 4.8 K is seen in the southern peak at $V = 1080\text{--}1180 \text{ km s}^{-1}$. Within 5" of the core radio source, there also exists a weak CO peak. The reality of this feature is questionable since it appears at the 4 σ level in just four channels (centered on 1134 km s^{-1}).

a) Kinematics

The velocity contours shown in Figure 2 exhibit an ordered structure with lowest velocity to the east and highest radial velocity to the west. The full range of emission within the ring is 1060–1268 km s^{-1} . In general, the CO velocities agree well with the H α velocities mapped by Atherton, Reay, and Taylor (1985), and we find a *kinematic* major axis position angle of 82° for a systemic velocity of 1126 km s^{-1} (VLSR).

Using the inclination and position angle of the major axis suggested by Walker (1968), 40° and 55°, respectively, a least-squares fit was performed for circular rotation and radial expansion as a function of radius, with the data weighted proportional to the CO intensity at that grid cell. The results of this fit are presented in Table 1. The deduced average expansion velocity of 71 km s^{-1} is approximately one-half of the rotational velocity of 164 km s^{-1} , indicating that there are significant noncircular motions in the ring material for this adopted major axis position angle. If we do not require the ring to have the same major axis as the light distribution and set the line of nodes at 83°, then a circular velocity of 185 km s^{-1} is in order. This is consistent with the major axis position angle (80° ± 9°) deduced by Baldwin, Wilson, and

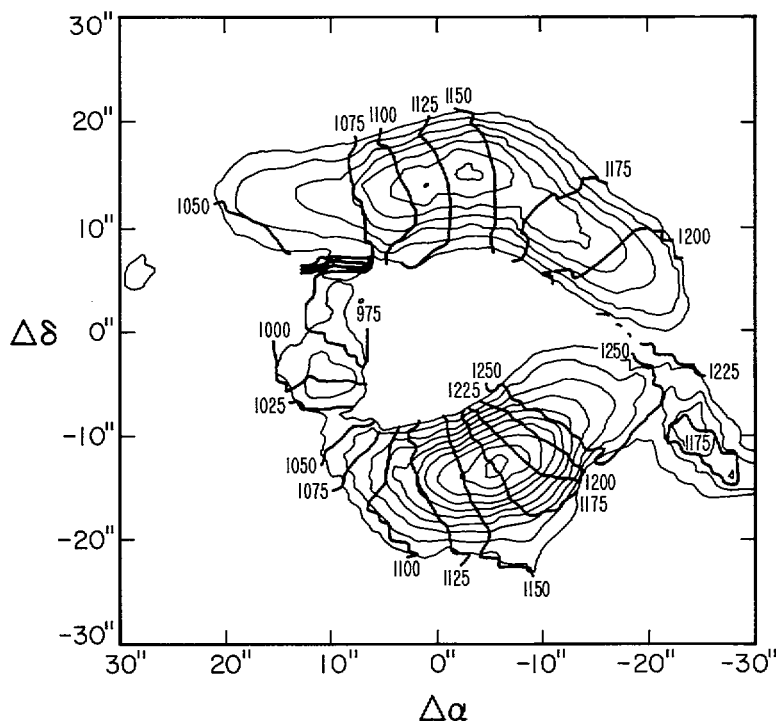


FIG. 2.—Contours of the CO velocity centroid for the emission between $V_{\text{LSR}} = 930\text{--}1320 \text{ km s}^{-1}$ are superposed on the convolved (7" x 11" resolution) interferometer map. Heliocentric velocities are 11 km s^{-1} higher. The contour interval is 20 Jy km s^{-1} per beam ($\Delta T_B = 1 \text{ K}$ corresponds to 0.94 Jy per beam), and the lowest contour is 40 Jy km s^{-1} per beam. The map center is the same as in Fig. 1.

TABLE 1
DERIVED PARAMETERS FOR RING

R (kpc)	$\langle R \rangle$ (kpc)	$\langle I_{\text{CO}} \rangle^a$ (K km s $^{-1}$)	V_{circ}^{-1} (km s $^{-1}$)	V_{exp}^{-1} (km s $^{-1}$)	$M_{\text{H}_2 + \text{He}}^b$ ($10^8 M_{\odot}$)
0–0.2	0.21	7	0.1
0.3–0.6	0.43	5	0.3
0.6–0.9	0.86	1	0.1
0.9–1.2	1.08	21	202	89	3.1
1.2–1.5	1.36	49	194	72	9.4
1.5–1.8	1.65	56	157	65	11.5
1.8–2.1	1.94	48	146	70	13.1
2.1–2.4	2.23	21	113	65	6.7
2.4–2.7	2.52	5	1.8
2.7–3.0	2.83	1	0.4
Weighted mean for $R = 0.9\text{--}2.4$	1.65	39	164	71	...

NOTE.—Circular and expansion velocities were obtained from an intensity-weighted least-squares fit to the emission within each annulus. Estimates are not given for annuli with too little emission to provide a reliable fit. We assume an inclination of 40° , a PA of the major axis of 55° , and a distance of 18.1 Mpc.

^aFace-on CO emission integral (i.e., corrected for inclination).

^bIncludes a factor of 1.36 correction to include He.

Whittle (1987) based on the emission-line kinematics throughout the disk at greater than $10''$ radius. In our discussion below, we take the point of view that the major axis really is at $\sim 55^\circ$ as indicated by the light distribution but caution that the deduced expansion of the molecular ring is entirely dependent on this assumption.

b) H_2 Mass

The total mass of molecular gas seen in the ring feature may be estimated using the relation between CO emission and molecular mass derived from observations of giant molecular clouds in the disk of the Milky Way. For transformation from the integrated CO emission to total H_2 mass, we use a constant of proportionality given by $N_{\text{H}_2}/I_{\text{CO}} = 3.6 \times 10^{20} \text{ cm}^{-2} (\text{K km s}^{-1})^{-1}$ (cf. Scoville and Sanders 1986). The total H_2 mass in the ring ($0.9 \leq R < 2.4$ kpc) is approximately $3.2 \times 10^9 M_{\odot}$, or a total mass of $4.4 \times 10^9 M_{\odot}$ allowing a factor of 1.36 for He. This H_2 mass estimate is nearly a factor of 10 greater than that obtained for the same region of our own Galaxy.

The peak column density in the southern peak is approximately $8 \times 10^{22} \text{ H}_2 \text{ cm}^{-2}$, corresponding to $A_v = 90$ mag for a standard gas-to-dust ratio ($1.9 \times 10^{21} \text{ H mag}^{-1}$; Bohlin, Savage, and Drake 1978). Our upper limit to the CO emission in the direction of the core source corresponds to a column density $< 5 \times 10^{21} \text{ H}_2 \text{ cm}^{-2}$ corresponding to $A_v \leq 5$ mag. This limit on the extinction is consistent with the reddening derived from near-infrared spectroscopy of the nucleus (Hall *et al.* 1981).

IV. DISCUSSION

The confinement of a large fraction of the molecular gas to a narrow ring is unusual for the gas distribution in galactic nuclei, at least in those that have been studied through CO interferometry. IC 342, NGC 6946, and NGC 253, which are Scd spirals, exhibit barlike structures with no evidence of voids at their centers (Lo *et al.* 1984; Ball *et al.* 1985; Canzian

et al. 1986). Although the Milky Way may also have a molecular cloud ring at $R \approx 250$ pc, both the mass of gas in this ring and the fraction of the total gas content it contains are much less than that in NGC 1068 (cf. Scoville 1972). (A small amount of neutral gas is apparently present within the inner 3.5 pc of NGC 1068 since Claussen and Lo 1986 detect a $350 L_{\odot} \text{ H}_2\text{O}$ maser at this position, and shocked H_2 emission is also seen in the central $4''$ Hall *et al.* 1981.)

a) Dynamics of the Ring

There are two viable explanations for the peculiar molecular gas kinematics of NGC 1068: (1) activity in the nuclear region has driven gas outward in an expanding ring; or (2) the ring is a dynamical structure resulting from a nonaxisymmetric gravitational potential such as a bar. If the ring is the result of nuclear activity, then the observed kinetic energy of 2×10^{56} ergs and momentum of $6.2 \times 10^{49} \text{ dyn s}^{-1}$ must have been provided by the responsible mechanism over a time scale less than 2×10^7 yr—the expansion time for 1.6 kpc at 71 km s^{-1} . A single event of this magnitude is rather unlikely; however, it is interesting to note that if the bulk of the $1.5 \times 10^{11} L_{\odot}$ attributed to star formation in the inner disk arises from early B stars as suggested by Wynn-Williams, Becklin, and Scoville (1985), the mean supernova rate would be $\sim 0.2 \text{ yr}^{-1}$, and the total energy supplied over the lifetime of the ring is an order of magnitude greater than the expansion energy—allowing for a low efficiency ($\sim 10\%$) deposition of energy into bulk motion within the disk. In any event, it is difficult to imagine explosive acceleration of the gas without dissociation and/or ionization.

Acceleration due to the action of a supersonic jet on the gas clouds might be less destructive, though it is difficult to impart enough momentum in this manner. Pedlar *et al.* (1983) estimate an equipartition pressure of $5 \times 10^{-9} \text{ dyn cm}^{-2}$ in the radio lobe (component A; $d \approx 100$ pc) closest to the NE “arm” of the ring. The momentum that this pressure could provide over 2×10^7 yr is less than 0.5% of the outward

momentum inferred for the molecular ring. In addition, it is doubtful that either a supernova or jet-driven ring would maintain the relatively coherent structure that is observed, since one might expect the former to result in a chaotic system of bubbles and filaments, and the latter to exhibit some deformation near the jet position angle.

b) *The Central Bar in NGC 1068*

We consider the most plausible scenario to be one in which the ring is the result of a barlike or oval gravitational potential. Optical photographic plates in the V band show the existence of both inner 0.5×0.35 and outer 5.0×4.5 rings (de Vaucouleurs, de Vaucouleurs, and Corwin 1976; Hodge 1968), possible signposts of a bar. Recent $2 \mu\text{m}$ mapping by Neugebauer *et al.* (1987) reveals an extremely high-contrast barlike structure extending to $\pm 16''$ radius at PA $\approx 45^\circ$.

Numerical simulations predict that a rotating stellar bar will sweep gas from the central region of the disk (as well as draw gas from outer regions) into an elliptical ringlike structure at the ends of the bar (cf. Huntley 1980), a picture consistent with the observed morphology of NGC 1068. The models of Combes and Gerin (1985), involving the evolution of molecular clouds in a stellar bar potential, similarly generate elliptical rings at the inner Linblad resonances. The shape, location, and velocity structure of the rings produced in these models are dependent on the relative angular velocities of the bar and gas, as well as the nature of the interactions allowed (e.g., gravitation only, self-gravitation, viscosity, formation of stars), and direct comparison with observation is difficult; the noncircular motion of the gas in NGC 1068 deduced from our observations is highly suggestive, however. It is noteworthy that Atherton, Reay, and Taylor (1985) infer the presence of a bar on the basis of the H α velocity field.

The column density of molecular gas in the inner $R \leq 1.0$ kpc is seen to be less than one-tenth of the peak ring density, that is $H_{\text{H}_2} < 8 \times 10^{21} \text{ cm}^{-2}$ or $M_{\text{H}_2}(R \leq 1 \text{ kpc}) < 4 \times 10^8 M_\odot$. The lack of gas in the central region is puzzling, since most simulations predict the formation of bars in the molecular gas alongside the stellar bar (in addition to the previously mentioned rings). Indeed, this seems to be the case in such galaxies as IC 342, NGC 6946, and NGC 253. However, it is likely that the intense burst of star formation that has blanketed the inner disk would have used up much of the gas available and dispersed the remainder.

c) *Origin of the Gas in the Inner Disk*

In addition to the problem of the origin of the ring structure, we are faced with explaining the existence of $3.2 \times 10^9 M_\odot$ of H $_2$ in the inner few kiloparsecs of NGC 1068. Studies of CO in the Virgo cluster spirals (cf. Young 1984) yield H $_2$ masses for the inner 5 kpc of around $5 \times 10^8 M_\odot$ for "average" galaxies to as much as $1.7 \times 10^9 M_\odot$ for the most gas-rich. Similarly, an H I mass of $6.6 \times 10^9 M_\odot$ is given for

the entirety of NGC 1068 (Huchtmiert and Seiradakis 1985) while for a set of comparison galaxies compiled by Giovanelli and Haynes (1983), we find a range of 2×10^9 to $3.2 \times 10^{10} M_\odot$. Thus, it appears that NGC 1068 possesses an unusually large amount of molecular gas in its central regions, but an average amount of atomic plus molecular hydrogen overall. This suggests that the 1.6 kpc ring is made of gas brought to the inner arm region by the action of the bar and compressed to form large molecular clouds. On the other hand, the bar appears to be made of an older stellar population, while the central disk is filled with young stars with ages on the order of 10^7 yr.

It is more plausible that a recent ($< 10^8$ yr ago) event delivered a large amount of gas to the nucleus of NGC 1068. This gas triggered a burst of massive star formation and then settled into the spiral arm structure under the influence of the bar. It is interesting to note that NGC 1068 is a member of a group including six other bright NGC galaxies (Condon *et al.* 1982) and NGC 1055 is only 15' W of NGC 1068 (see Burbidge, Burbidge, and Prendergast 1959). Another possibility is that NGC 1068 has merged with a small companion galaxy; the disruption caused by this capture might then trigger the gas infall. We must point out, however, that there is little additional evidence, such as H I tidal tails and arcs, to point toward a galaxy-galaxy encounter, but the circumstantial evidence is suggestive.

We would also like to point out that the role of the active nucleus in the formation of the H $_2$ rings is probably negligible. It is likely, however, that the central engine is fueled, and was possibly created, by the same event that caused the star formation burst and led to the ring. Much of the extended radio emission lies along the projected bar major axis and may be due to supernovae in the bar environment (see also van der Hulst, Hummel, and Dickey 1982).

V. CONCLUSIONS

High-resolution interferometer maps of the CO emission in NGC 1068 have shown that the bulk of the molecular gas is confined to a ring approximately 1.6 kpc in radius situated at the outer edge of the active star forming disk. The observed noncircular motions and peculiar distribution of these neutral gas clouds are probably due to the presence of a stellar bar in the center of NGC 1068. The high mass of molecular gas in the central $R \leq 5$ kpc could be the result of an encounter with a companion or cannibalism of a dwarf galaxy. The role of the active nucleus and radio jet upon the kinematics of the neutral gas appears to be negligible.

We acknowledge the major contributions of the staff at the Owens Valley Radio Observatory in the construction, development, and operation of the millimeter-wave interferometer. It is also a pleasure to thank P. Goldreich, D. Sanders, and S. Simkin for discussions. This research was supported in part by NSF grant AST 84-12473.

REFERENCES

- Atherton, P. D., Reay, N. K., and Taylor, K. 1985, *M.N.R.A.S.*, **216**, 17P.
 Baldwin, J., Wilson, A. E., and Whittle, M. 1986, *Ap. J.*, submitted.
 Ball, R., Sargent, A. I., Scoville, N. Z., Lo, K. Y., and Scott, S. L. 1985, *Ap. J. (Letters)*, **298**, L21.
 Bohlin, R. C., Savage, B. D., and Drake, J. F. 1978, *Ap. J.*, **224**, 132.
 Burbidge, E. M., Burbidge, G. R., and Prendergast, K. H. 1959, *Ap. J.*, **130**, 26.
 Canizares, B., Mundy, L., and Scoville, N. Z. 1987, in preparation.
 Claussen, M. J., and Lo, K. Y. 1986, *Ap. J.*, **308**, 592.

- Combes, F., and Gerin, M. 1985, *Astr. Ap.*, **150**, 327.
 Condon, J. J., Condon, M. A., Gisler, G., and Puschell, J. J. 1982, *Ap. J.*, **252**, 102.
 de Vaucouleurs, G., de Vaucouleurs, A., and Corwin, H. G. 1976, *Second Reference Catalog of Bright Galaxies* (Austin: University of Texas).
 Giovanelli, R., and Haynes, M. P. 1983, *A.J.*, **88**, 881.
 Hall, D. N. B., Kleinmann, S. G., Scoville, N. Z., and Ridgway, S. G. 1981, *Ap. J.*, **248**, 898.
 Hodge, P. W. 1968, *Ap. J.*, **238**, 524.
 Huchtmeier, W. K., and Seirodakis, J. H. 1985, *Astr. Ap.*, **143**, 216.
 Huntley, J. M. 1980, *Ap. J.*, **238**, 524.
 Lo, K. Y., et al. 1984, *Ap. J. (Letters)*, **282**, L59.
 Neugebauer, G., Matthews, K., Soifer, B. T., and Scoville, N. Z. 1987, in preparation.
 Pedlar, A., Booler, R. V., Spencer, R. E., and Stewart, O. J. 1983, *M.N.R.A.S.*, **202**, 647.
 Sandage, A., and Tammann, G. A. 1975, *Ap. J.*, **196**, 313.
 Sanders, D. B., Scoville, N. Z., Young, J. S., Soifer, B. T., Schloerb, F. P., Rice, W. L., and Danielson, G. E. 1986, *Ap. J. (Letters)*, **305**, L45.
 Scoville, N. Z. 1972, *Ap. J. (Letters)*, **175**, L127.
 Scoville, N. Z., and Sanders, D. B. 1986, in *Interstellar Processes*, ed. H. A. Thronson and D. Hollenbech (Dordrecht: Reidel), in press.
 Scoville, N. Z., Sanders, D. B., and Clemens, D. P. 1986, *Ap. J. (Letters)*, **310**, L77.
 Scoville, N. Z., Young, J. S., and Lucy, L. B. 1983, *Ap. J.*, **270**, 443.
 Soifer, B. T., Sanders, D. B., Neugebauer, G., Danielson, G. E., Lonsdale, C. J., Madore, B. F., and Persson, S. E. 1986, *Ap. J. (Letters)*, **303**, L41.
 Telesco, C. M., Becklin, E. E., Wynn-Williams, C. G., and Harper, D. A. 1984, *Ap. J.*, **282**, 427.
 Ulich, B. L. 1981, *A.J.*, **86**, 1619.
 Ulvestad, J. S., Neff, S. G., and Wilson, A. S. 1986, *A.J.*, in press.
 van der Hulst, J. M., Hummel, E., and Dickey, J. M. 1982, *Ap. J. (Letters)*, **261**, L59.
 Walker, M. F. 1968, *Ap. J.*, **151**, 71.
 Wilson, A. S., and Ulvestad, J. S. 1983, *Ap. J.*, **275**, 8.
 Wynn-Williams, C. G., Becklin, E. E., and Scoville, N. Z. 1985, *Ap. J.*, **297**, 607.
 Young, J. S. 1984, in *ESO Workshop on the VIRGO Cluster*, ed. O.-G. Richter and B. Binggeli (Munich: ESO), p. 151.

S. T. MYERS and N. Z. SCOVILLE: Department of Astronomy, 105-24, California Institute of Technology, Pasadena, CA 91125

1987APU...312I..39M

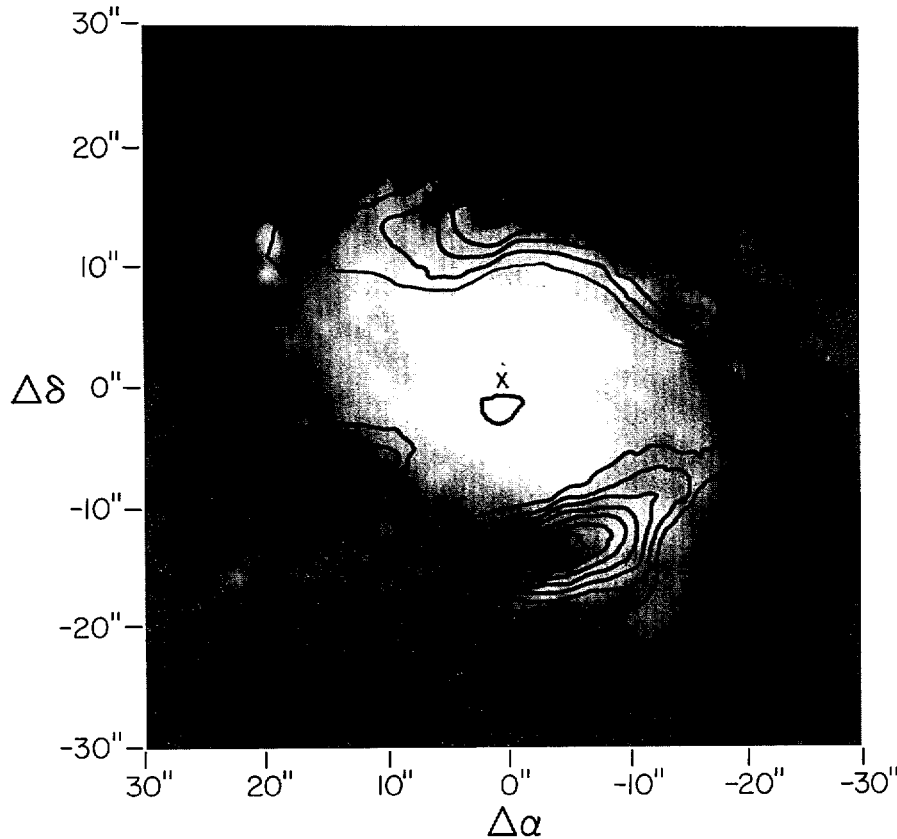


FIG. 1a

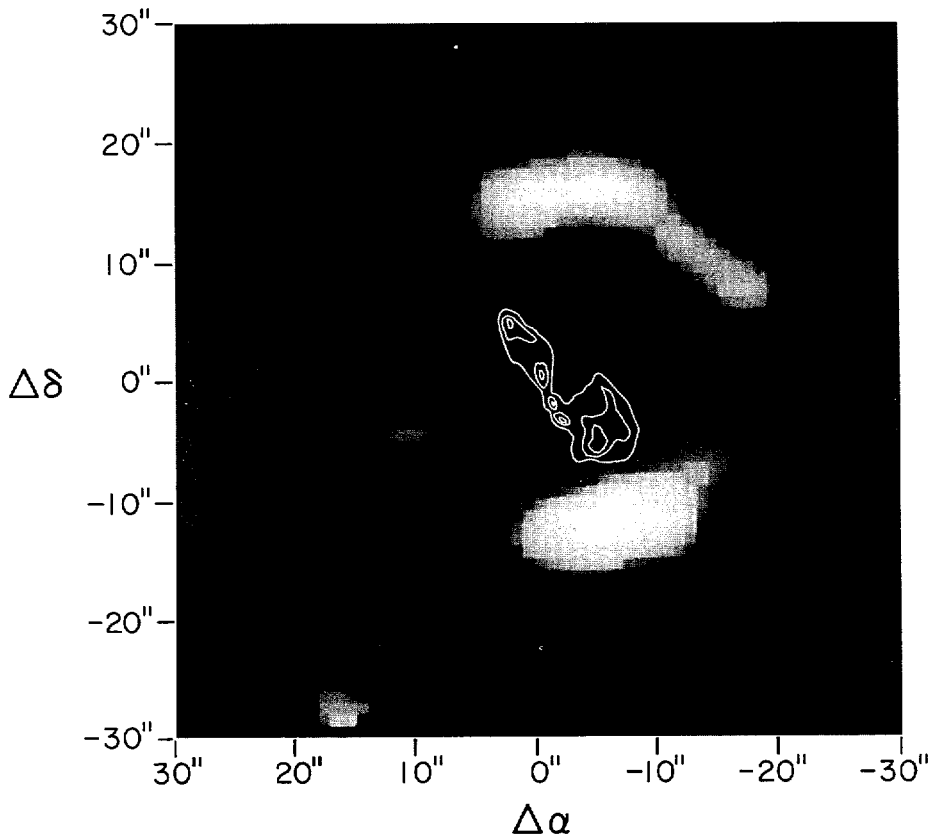


FIG. 1b

FIG. 1.—Contours of the integrated CO emission mapped by the interferometer at $5'' \times 7''$ resolution are shown in the upper panel superposed on an optical r band image provided by J. MacKenty obtained on the University of Hawaii 2.3 m telescope. The contour interval is 20 Jy km s^{-1} per beam ($\Delta T_B = 1 \text{ K}$ corresponds to 0.43 Jy per beam); the lowest contour is 20 Jy km s^{-1} per beam). In the lower panel (b), the $\lambda = 6 \text{ cm}$ radio continuum emission ($0'.4 \times 0'.4$ resolution) is shown as white contours superposed on a gray scale representation of the CO emission. The optical nucleus coincides with the bright, central peak in the VLA map (Wilson and Ulvestad 1983). The centers of both maps are at R.A. = $2^{\text{h}}40^{\text{m}}7^{\text{s}}076$, decl. = $-0^{\circ}13'31''.48$ (1950).